Atmos. Chem. Phys. Discuss., 15, 26067–26088, 2015
www.atmos-chem-phys-discuss.net/15/26067/2015/
doi:10.5194/acpd-15-26067-2015


Atmospheric Chemistry and Physics Discussions



# Observations of fluorescent aerosol–cloud interactions in the free troposphere at the Sphinx high Alpine research station, Jungfraujoch

**I. Crawford[1], G. Lloyd[1,2], K. N. Bower[1], P. J. Connolly[1], M. J. Flynn[1], P. H. Kaye[3], T. W. Choularton[1], and M. W. Gallagher[1]**

[1]Centre for Atmospheric Science, SEAES, University of Manchester, Manchester, UK
[2]NCAS, National Centre for Atmospheric Science, University of Manchester, UK
[3]Science and Technology Research Institute, University of Hertfordshire, UK

Received: 31 July 2015 – Accepted: 5 September 2015 – Published: 25 September 2015

Correspondence to: I. Crawford (i.crawford@manchester.ac.uk)

Published by Copernicus Publications on behalf of the European Geosciences Union.







## Abstract

The fluorescent nature of aerosol at a high Alpine site was studied using a wide-band integrated bioaerosol (WIBS-4) single particle multi-channel ultra violet-light induced fluorescence (UV-LIF) spectrometer. This was supported by comprehensive cloud microphysics and meteorological measurements with the aims of cataloguing concentrations of bio-fluorescent aerosols at this high altitude site and also investigating possible influences of UV-fluorescent particle types on cloud–aerosol processes. Analysis of background free tropospheric air masses, using a total aerosol inlet, showed there to be a minor but statistically insignificant increase in the fluorescent aerosol fraction during in-cloud cases compared to out of cloud cases. The size dependence of the fluorescent aerosol fraction showed the larger aerosol to be more likely to be fluorescent with 80 % of 10 µm particles being fluorescent. Whilst the fluorescent particles were in the minority ($N_{Fl}/N_{All} = 0.27 \pm 0.19$), a new hierarchical agglomerative cluster analysis approach, Crawford et al. (2015) revealed the majority of the fluorescent aerosol were likely to be representative of fluorescent mineral dust. A minor episodic contribution from a cluster likely to be representative of primary biological aerosol particles (PBAP) was also observed with a wintertime baseline concentration of $0.1 \pm 0.4\,L^{-1}$. Given the low concentration of this cluster and the typically low ice active fraction of studied PBAP (e.g. *pseudomonas syringae*) we suggest that the contribution to the observed ice crystal concentration at this location is not significant during the wintertime.

## 1 Introduction

The formation of cloud particles and their subsequent interactions with the atmosphere are highly uncertain, with the formation and evolution of mixed phase and glaciated clouds being poorly understood (Penner et al., 2001). Improving our understanding of primary ice nucleation is critical in underpinning these uncertainties as even modest concentrations of primary ice can result in the rapid glaciation and subsequently





ACPD
15, 26067–26088, 2015



cause precipitation in mixed phase clouds, drastically changing cloud lifetime (Lloyd et al., 2015; Crawford et al., 2012; Crosier et al., 2011). Many candidate aerosol have been assessed for their heterogeneous ice nucleating ability with a particular emphasis being placed on mineral dust and primary biological aerosols. The ice nucleating efficiency of many naturally occurring and surrogate dust aerosols have been investigated and they are generally considered to be efficient ice nuclei with observations of ice activation occurring over water subsaturated and supersaturated conditions at temperatures below −10 °C (Hoose and Möhler, 2012). The influence of accumulated coatings through atmospheric processing have also been assessed where it was found these act to significantly increase the saturation ratio required for ice nucleation, effectively deactivating an otherwise ice active mineral dust. Saharan desert dust was observed during an experiment in a Florida region where it was suggested that the dust may have been acting as an effective high temperature ice nucleus resulting in the observed glaciation of an altocumulus cloud at −5 °C (Sassen et al., 2003). Saharan desert dust was also found to be the major non-volatile component of ice crystal residuals in cirrus over the Alps (Heintzenberg et al., 1996). The high ice nucleation efficiency of mineral dusts and their capacity for long-range transport therefore make them a potentially potent component in the formation and modification of clouds worldwide. Certain Primary Biological Aerosol Particles exhibit the ability to nucleate ice and it has recently been suggested that ice active PBAP may have evolved over geological time scales to enhance rainfall, fostering an environment beneficial to the growth of plants and microorganisms through the so-called bioprecipitation feedback cycle (Morris et al., 2014). A small number of bacterial strains, fungal spores and rusts have been identified as ice active at temperatures warmer than −10 °C due to the presence of an ice nucleating protein in the outer cell wall which is structurally similar to ice, facilitating ice growth (Kajava and Lindow, 1993; Govindarajan and Lindow, 1988; Hoose and Möhler, 2012). However, of the ice active bacterial strains studied so far only a small fraction nucleates ice at very warm temperature, e.g. Möhler et al. (2008) demonstrated *Pseudomonas syringae* have a maximum ice active fraction of 0.005 at −9.7 °C, how-





ACPD
15, 26067–26088, 2015



ever, they may still play a significant role in the formation and modification of cloud as plant surface derived bacterial aerosol can be transported to the higher levels of the atmosphere in high concentrations as a result of heavy rainfall and storm generated uplift (Crawford et al., 2014; DeLeon-Rodriguez et al., 2013; Huffman et al., 2013). The Sphinx high Alpine research station Jungfraujoch has hosted several intensive measurement campaigns to study cloud aerosol interactions. Previous measurements at the site have found there to be an enhancement of mineral dust in cloud particle residuals compared to interstitial aerosol measurements (Kamphus et al., 2010). This study also deployed a portable ice nucleation chamber during June 2009, where two Saharan Dust Events (SDE) were reported. During the SDE it was found that ice nucleus concentrations were correlated with larger aerosol ($D > 0.5\,\mu m$) with reported deposition mode ice nuclei concentrations of up to several hundred per litre. This is discussed in more detail in the companion paper to this study by Lloyd et al. (2015). In this study we present contemporaneous aerosol and cloud microphysics measurements at the same site to characterise the fluorescent constituents of aerosol and their possible role in cloud processes.

## 2 Methods

### 2.1 Site description

During January and February 2014 the Ice NUcleation Process Investigation And Quantification (INUPIAQ) project was conducted at the high Alpine research station Jungfraujoch (JFJ, 3580 m a.s.l.; 46.55° N, 7.98° E) in Switzerland to investigate the influence of a range of aerosol types on ice crystal number concentration alongside secondary ice processes in natural supercooled cloud. The JFJ site is enveloped by cloud for approximately 37 % of the year making it ideal for studying cloud–aerosol interactions, with the site residing in the free troposphere during the wintertime (Baltensperger et al., 1998).





ACPD
15, 26067–26088, 2015



## 2.2 Instrumentation and inlets

Fluorescent aerosol number size distributions were measured using a Wideband Integrated Bioaerosol Spectrometer (WIBS, Version 4, University of Hertfordshire) on a single particle basis and designed primarily for identifying biofluorphores. A full technical description can be found in Kaye et al. (2005), while various applications and analysis approaches including monitoring at high altitude sites can be found in Gabey et al. (2013); Stanley et al. (2011) and Crawford et al. (2014). A brief description of the instrument is now given. The WIBS-4 spectrometer exploits the principle of UV light induced fluorescence where a particle of interest is excited with UV radiation and the resultant fluorescence is detected, with fluorescence being an indicator that the particle may be biological. In the WIBS-4 aerosol is drawn into the sample volume and illuminated by a 635 nm laser and the resultant forward scattered light is used determine the particle size and shape using a quadrant detector. Side scattered light is collected and sequentially triggers two xenon flash lamps, filtered to excite the sampled particle at 280 and 370 nm respectively. The first lamp is pulsed and the resultant fluorescence is collected, filtered and passed to two fluorescence detectors. The detectors are filtered to measure fluorescence over two bands (320–400 and 410–650 nm) which are then recorded. The second flash lamp is then triggered and the fluorescence detected by the 2nd band is recorded. The whole process takes approximately 25 µs and the instrument has a maximum particle analysis rate of 125 particles $s^{-1}$. This provides three measurements of particle fluorescence over two excitation wavelengths, particle size and an approximation of particle shape, all on a single particle basis. The excitation and detection wavelengths have been selected to conform to known auto-fluorescence bands of common components of biological materials (e.g. proteins, tryptophan and Nicotinamide adenine dinucleotide, NADH, the latter related to cell metabolism) such that they can be discriminated from non-biological, non-fluorescent particles. Due to detector sensitivity and background fluorescence within the WIBS-4 optical chamber both the fluorescence of aerosol with diameters $D_p < 0.8$ µm cannot be accurately mea-





ACPD
15, 26067–26088, 2015



sured, and the counting efficiency decreases, Gabey et al. (2011). Therefore the analysis presented here is limited to aerosols with diameters greater than 0.8 µm, unless otherwise stated. Whilst WIBS-4 instruments have many advantages over traditional UV-LIF spectrometers, limitations include difficulties in discriminating different classes of biological classes unambiguously and fluorescent non-biological aerosols must be identified. Fluorescence of some mineral dusts was examined by Pöhlker et al. (2012) who characterised their weak fluorescence properties allowing them to be generally discriminated from common PBAP using UV-LIF. In this study we use a new hierarchical agglomerative data processing method for WIBS-4 UV-LIF measurements to discriminate between particle types. A detailed discussion of this can be found in Crawford et al. (2015).

The WIBS-4 sampled from a total inlet (TI) which is now described. The TI samples all particles with $D_p < 40\,\mu m$ and for wind speeds $< 20\,m\,s^{-1}$. The sampled air is first heated to +20 °C, evaporating droplets and ice crystals such that their residuals are sampled along with any interstitial aerosol (Weingartner et al., 1999).

Comprehensive cloud microphysics measurements were made at the site and are described in Lloyd et al. (2015). In this study measurements of cloud droplet and ice crystal number concentrations were measured respectively with a Cloud Droplet Probe (CDP-100, Droplet Measurement Technologies, DMT), described by Lance et al. (2010), and a 3 View – Cloud Particle Imager (3V-CPI, a multi-probe comprising a 2-D stereo imaging spectrometer (2D-S) and Cloud Particle Imager (CPI), e.g. Lawson et al. (2015). The CDP-100 is an optical scattering spectrometer able to size particles in the range $2 < D_p < 50\,\mu m$ whilst the 3V-CPI is an integrated 2-D-Stereo (2DS) LED imaging spectrometer and Cloud Particle Imaging (CPI), CCD imaging spectrometer with resolutions of 10 and 2.3 µm respectively. These are capable of measuring ice particle size distributions between 10–1280 µm and able to discriminate particle habit (based on shape analysis) for particles greater than approximately 25–30 µm. Details of the analysis techniques used for these instruments are provided in Crosier et al. (2014); Lloyd et al. (2015).





ACPD
15, 26067–26088, 2015



## 3 Results

During the experiment there were two extended Saharan dust events (00:00 CET, 1 February–00:00 CET, 2 February and 04:30 CET, 18 February–19:00 CET, 19 February). In this paper we focus on the period outside these events in order to characterise the behaviour of high Alpine fluorescent aerosol under typical winter time background conditions. Discussion of the SDE's will be described elsewhere. 5 min integration periods are used in all analysis unless otherwise stated.

### 3.1 Meteorological conditions

An overview of the meteorological conditions at the JFJ site over the background period 6–18 February is provided in Fig. 1. Average temperatures of $-11.3 \pm 4.3$ and $-14.6 \pm 3.3\,^{\circ}\mathrm{C}$ were reported for out of cloud and in cloud periods respectively with wind speeds of $5.2 \pm 3.3\,\mathrm{m\,s^{-1}}$. Daily HYSPLIT back trajectory analysis (Fig. 2) showed the majority of air masses to have passed over the Atlantic ocean in the preceding 72 h during this period. Analysis of wind speed and direction shows the highest concentrations of fluorescent aerosols occur when the wind is coming from the south east for wind speeds in excess of $15\,\mathrm{m\,s^{-1}}$, i.e. coincident with flow up from the Aletsch glacier.

### 3.2 Background observations of fluorescent aerosol

The period between the two SDE is considered representative of the typical background aerosol concentrations at the site during the wintertime. Average out of cloud total coarse aerosol, $N_{\mathrm{All}}$, and total fluorescent aerosol concentrations, $N_{\mathrm{Fl}}$, measured by the WIBS-4 were $30.6 \pm 19.3$ and $6.3 \pm 5.7\,\mathrm{L^{-1}}$ respectively for the period 6–18 February, as shown in Fig. 3 (5 min averages).

To investigate the potential interaction of fluorescent aerosol with clouds we have studied the fluorescent aerosol concentration fraction ($N_{\mathrm{Fl}}/N_{\mathrm{All}}$) over different temperature regimes for out of cloud, mixed phase and glaciated conditions as summarised





ACPD
15, 26067–26088, 2015



in Fig. 4. Here we define out of cloud as all periods where the total water content (TWC) is less than 0.01 g m$^{-3}$; mixed phase as all periods where the TWC ≥ 0.01 g m$^{-3}$ and ice mass fraction (IMF) is less than 0.5; and glaciated as all periods where TWC ≥ 0.01 g m$^{-3}$ and IMF ≥ 0.5. It can be seen across all temperature regimes that the average in-cloud fluorescent aerosol fractions were slightly greater (∼ 0.28, all temperatures) than for out of cloud conditions (∼ 0.24, all temperatures), however the variations are large and the mean values of each case lie within one standard deviation of each other with no one case proving to be statistically significant. It was also observed that the fluorescent aerosol fraction decreases with decreasing temperature.

Figure 5 shows the fluorescent aerosol fraction for cloud events persisting for a minimum of 30 min in duration with mean, minimum and maximum observed average fluorescent aerosol fractions of 0.27 ± 0.12, 0.05 and 0.49 respectively over 34 separate cloud events. It can be seen that many of the clouds feature large variations in fluorescent aerosol fraction, while others have relatively little variation. No apparent trend is observed between the mean fluorescent aerosol fractions and contemporaneous mean meteorological or cloud microphysical parameters, suggesting that particle fluorescence does not impact cloud evolution or formation. The majority of cloud events occur in the $-15 \leq T < -10$ °C regime: Fig. 6 shows the average fluorescent and non-fluorescent particle size distributions for out of cloud, mixed phase and glaciated conditions in this temperature regime. In each case the single mode of the distribution occurs at 0.58 µm. Figure 7 shows the size dependence of the fluorescent aerosol fraction for the three studied temperature regimes for out of cloud, mixed phase and glaciated conditions. In each case it was observed that the fluorescent aerosol fraction increases with size, with approximately 80 % of 10 µm particles being fluorescent in nature, with the fluorescent aerosol fraction decreasing to approximately 20 % for 1 µm particles.





ACPD
15, 26067–26088, 2015



## 4 Analysis of fluorescent aerosol characteristics

To probe the nature of the fluorescent aerosols the single particle data from the period 6–18 February (approximately 27 000 fluorescent particles) was clustered using the Ward hierarchical agglomerative cluster analysis linkage and $Z$ score normalisation technique with the log of the size and particle asymmetry factors used to improve the symmetry of the cluster distribution. For further details on the hierarchical agglomerative cluster analysis method used here see Crawford et al. (2015). The Calinski–Harabasz metric was used to determine the optimum cluster solution to retain, returning a 3 cluster solution as shown in Fig. 8. Clusters 1 and 2 were the dominant clusters, both of which display weak fluorescence which is characteristic of mineral dust (Pöhlker et al., 2012). The sum of particle concentrations from both clusters 1 and 2 correlated well with the total fluorescent particle concentration ($N_{cl1+cl2}$) = 0.3 + 0.94 × $N_{Fl}$, $r^2$ = 0.99). Cluster 3 displayed significantly higher fluorescence in all 3 channels suggesting that this was likely representative of biological material (Crawford et al., 2014). However, periods during which cluster 3 particles appeared were sparse with typical average concentrations over the period of $0.1 \pm 0.4\,L^{-1}$ observed. Very occasional episodic events with maximum concentrations reaching of the order of a few per litre were observed. We would expect lower concentrations of local PBAP in the wintertime at this site due to reduced surface sources of seasonal PBAP coupled with an annual minimum in planetary boundary layer (PBL) height which would allow for very little in the way of PBL influenced air to reach the research station (Ketterer et al., 2014; Collaud Coen et al., 2011; Nyeki et al., 1998). In summary the majority of fluorescent aerosol sampled at the site during these periods is likely non-biological in nature with only minor episodic contributions from bioaerosols. Such low concentrations of PBAP are unlikely to have any significant impact on cloud evolution through ice nucleation due to the low ice active fractions reported for typical PBAP; e.g. assuming the cluster is representative of *Pseudomonas syringae* (Möhler et al., 2008) this would





ACPD
15, 26067–26088, 2015



yield an IN concentration of only $5 \times 10^{-4}\,L^{-1}$ which is several orders of magnitude less than the reported ice crystal concentration (Lloyd et al., 2015).

## 5 Summary and conclusions

Analysis of 288 h of contemporaneous aerosol fluorescence and cloud microphysics measurements made during wintertime background conditions at a high Alpine site revealed that the majority of aerosol sampled with a WIBS-4 UV-LIF spectrometer were non-fluorescent with only 27 % of the aerosol displaying fluorescence. We investigated the potential links between aerosol fluorescence and cloud microphysics both in general and for 34 individual cloud events persisting for at least 30 min and we report that there was no apparent link between the fluorescent aerosol fraction and observed cloud microphysical parameters and meteorology, suggesting that aerosol fluorescence does not influence cloud formation/evolution at the site.

We observed that particle fluorescence is a strong function of size with 80 % of 10 µm particles displaying fluorescence, decreasing to 20 % at 1 µm. Hierarchical agglomerative cluster analysis of the fluorescent particles yielded a three cluster solution: two of the clusters displayed fluorescent characteristics consistent with fluorescent mineral dust and these clusters accounted for approximately 95 % of the observed fluorescent particles. The remaining cluster was moderately fluorescent in all three channels and is assumed to be biological in origin. Concentrations of the assumed PBAP cluster were sparse, occurring in occasional minor episodes with a baseline concentration of $0.1 \pm 0.4\,L^{-1}$. Given the low concentration of this cluster and the typically low ice active fraction of studied PBAP (e.g. *Pseudomonas syringae*, Möhler et al., 2008) we suggest that the contribution to the observed ice crystal concentration at this location is not significant during the wintertime, however, analysis of wind speed and direction suggests that large sources from the Po valley region may advect up the Aletsch glacier during periods of high wind speed which may be of significance during the summer when the





ACPD
15, 26067–26088, 2015



PBL is higher. We suggest that longer term data sets are required to examine this in detail.

*Acknowledgements.* This work was funded by the NERC INUPIAQ programme, grant number NE/K006002/1. The data used in this manuscript can be accessed from the British Atmospheric Data Centre. HYPLIT data was obtained from the NOAA Air Resource Laboratory (http://ready.arl.noaa.gov/).

## References

Baltensperger, U., Schwikowski, M., Jost, D. T., Nyeki, S., Gaggeler, H. W., and Poulida, O.: Scavenging of atmospheric constituents in mixed phase clouds at the high-alpine site Jungfraujoch part I: Basic concept and aerosol scavenging by clouds, Atmos. Environ., 32, 3975–3983, 1998. 26070

Collaud Coen, M., Weingartner, E., Furger, M., Nyeki, S., Prévôt, A. S. H., Steinbacher, M., and Baltensperger, U.: Aerosol climatology and planetary boundary influence at the Jungfraujoch analyzed by synoptic weather types, Atmos. Chem. Phys., 11, 5931–5944, doi:10.5194/acp-11-5931-2011, 2011. 26075

Crawford, I., Bower, K. N., Choularton, T. W., Dearden, C., Crosier, J., Westbrook, C., Capes, G., Coe, H., Connolly, P. J., Dorsey, J. R., Gallagher, M. W., Williams, P., Trembath, J., Cui, Z., and Blyth, A.: Ice formation and development in aged, wintertime cumulus over the UK: observations and modelling, Atmos. Chem. Phys., 12, 4963–4985, doi:10.5194/acp-12-4963-2012, 2012. 26069

Crawford, I., Robinson, N. H., Flynn, M. J., Foot, V. E., Gallagher, M. W., Huffman, J. A., Stanley, W. R., and Kaye, P. H.: Characterisation of bioaerosol emissions from a Colorado pine forest: results from the BEACHON-RoMBAS experiment, Atmos. Chem. Phys., 14, 8559–8578, doi:10.5194/acp-14-8559-2014, 2014. 26070, 26071, 26075

Crawford, I., Ruske, S., Topping, D. O., and Gallagher, M. W.: Evaluation of hierarchical agglomerative cluster analysis methods for discrimination of primary biological aerosol, Atmos. Meas. Tech. Discuss., 8, 7303–7333, doi:10.5194/amtd-8-7303-2015, 2015. 26068, 26072, 26075

Crosier, J., Bower, K. N., Choularton, T. W., Westbrook, C. D., Connolly, P. J., Cui, Z. Q., Crawford, I. P., Capes, G. L., Coe, H., Dorsey, J. R., Williams, P. I., Illingworth, A. J., Gal-





ACPD
15, 26067–26088, 2015



lagher, M. W., and Blyth, A. M.: Observations of ice multiplication in a weakly convective cell embedded in supercooled mid-level stratus, Atmos. Chem. Phys., 11, 257–273, doi:10.5194/acp-11-257-2011, 2011. 26069

Crosier, J., Choularton, T. W., Westbrook, C. D., Blyth, A. M., Bower, K. N., Connolly, P. J., Dearden, C., Gallagher, M. W., Cui, Z., and Nicol, J. C.: Microphysical properties of cold frontal rainbands, Q. J. Roy. Meteor. Soc., 140, 1257–1268, doi:10.1002/qj.2206, 2014. 26072

DeLeon-Rodriguez, N., Lathem, T. L., Rodriguez-R, L. M., Barazesh, J. M., Anderson, B. E., Beyersdorf, A. J., Ziemba, L. D., Bergin, M., Nenes, A., and Konstantinidis, K. T.: Microbiome of the upper troposphere: species composition and prevalence, effects of tropical storms, and atmospheric implications, P. Natl. Acad. Sci. USA, 110, 2575–2580, doi:10.1073/pnas.1212089110, 2013. 26070

Gabey, A. M., Stanley, W. R., Gallagher, M. W., and Kaye, P. H.: The fluorescence properties of aerosol larger than 0.8 µm in urban and tropical rainforest locations, Atmos. Chem. Phys., 11, 5491–5504, doi:10.5194/acp-11-5491-2011, 2011. 26072

Gabey, A. M., Vaitilingom, M., Freney, E., Boulon, J., Sellegri, K., Gallagher, M. W., Crawford, I. P., Robinson, N. H., Stanley, W. R., and Kaye, P. H.: Observations of fluorescent and biological aerosol at a high-altitude site in central France, Atmos. Chem. Phys., 13, 7415–7428, doi:10.5194/acp-13-7415-2013, 2013. 26071

Govindarajan, A. G. and Lindow, S. E.: Size of bacterial ice-nucleation sites measured in situ by radiation inactivation analysis, P. Natl. Acad. Sci. USA, 85, 1334–1338, 1988. 26069

Heintzenberg, J., Okada, K., and Ström, J.: On the composition of non-volatile material in upper tropospheric aerosols and cirrus crystals, Atmos. Res., 41, 81–88, doi:10.1016/0169-8095(95)00042-9, 1996. 26069

Hoose, C. and Möhler, O.: Heterogeneous ice nucleation on atmospheric aerosols: a review of results from laboratory experiments, Atmos. Chem. Phys., 12, 9817–9854, doi:10.5194/acp-12-9817-2012, 2012. 26069

Huffman, J. A., Prenni, A. J., DeMott, P. J., Pöhlker, C., Mason, R. H., Robinson, N. H., Fröhlich-Nowoisky, J., Tobo, Y., Després, V. R., Garcia, E., Gochis, D. J., Harris, E., Müller-Germann, I., Ruzene, C., Schmer, B., Sinha, B., Day, D. A., Andreae, M. O., Jimenez, J. L., Gallagher, M., Kreidenweis, S. M., Bertram, A. K., and Pöschl, U.: High concentrations of biological aerosol particles and ice nuclei during and after rain, Atmos. Chem. Phys., 13, 6151–6164, doi:10.5194/acp-13-6151-2013, 2013. 26070





ACPD
15, 26067–26088, 2015



Kajava, A. V. and Lindow, S. E.: A model of the three-dimensional structure of ice nucleation proteins, J. Mol. Biol., 232, 709–717, doi:10.1006/jmbi.1993.1424, 1993. 26069

Kamphus, M., Ettner-Mahl, M., Klimach, T., Drewnick, F., Keller, L., Cziczo, D. J., Mertes, S., Borrmann, S., and Curtius, J.: Chemical composition of ambient aerosol, ice residues and cloud droplet residues in mixed-phase clouds: single particle analysis during the Cloud and Aerosol Characterization Experiment (CLACE 6), Atmos. Chem. Phys., 10, 8077–8095, doi:10.5194/acp-10-8077-2010, 2010. 26070

Kaye, P. H., Stanley, W. R., Hirst, E., Foot, E. V., Baxter, K. L., and Barrington, S. J.: Single particle multichannel bio-aerosol fluorescence sensor, Opt. Express, 13, 3583, doi:10.1364/OPEX.13.003583, 2005. 26071

Ketterer, C., Zieger, P., Bukowiecki, N., Collaud Coen, M., Maier, O., Ruffieux, D., and Weingartner, E.: Investigation of the planetary boundary layer in the Swiss Alps using remote sensing and in situ measurements, Bound.-Lay. Meteorol., 151, 317–334, doi:10.1007/s10546-013-9897-8, 2014. 26075

Lance, S., Brock, C. A., Rogers, D., and Gordon, J. A.: Water droplet calibration of the Cloud Droplet Probe (CDP) and in-flight performance in liquid, ice and mixed-phase clouds during ARCPAC, Atmos. Meas. Tech., 3, 1683–1706, doi:10.5194/amt-3-1683-2010, 2010. 26072

Lawson, R. P., Woods, S., and Morrison, H.: The microphysics of ice and precipitation development in tropical cumulus clouds, J. Atmos. Sci., 72, 2429–2445, doi:10.1175/JAS-D-14-0274.1, 2015. 26072

Lloyd, G., Choularton, T. W., Bower, K. N., Gallagher, M. W., Connolly, P. J., Flynn, M., Farrington, R., Crosier, J., Schlenczek, O., Fugal, J., and Henneberger, J.: The origins of ice crystals measured in mixed phase clouds at High-Alpine site Jungfraujoch, Atmos. Chem. Phys. Discuss., 15, 18181–18224, doi:10.5194/acpd-15-18181-2015, 2015. 26069, 26070, 26072, 26076

Möhler, O., Georgakopoulos, D. G., Morris, C. E., Benz, S., Ebert, V., Hunsmann, S., Saathoff, H., Schnaiter, M., and Wagner, R.: Heterogeneous ice nucleation activity of bacteria: new laboratory experiments at simulated cloud conditions, Biogeosciences, 5, 1425–1435, doi:10.5194/bg-5-1425-2008, 2008. 26069, 26075, 26076

Morris, C. E., Conen, F., Alex Huffman, J., Phillips, V., Pöschl, U., and Sands, D. C.: Bioprecipitation: a feedback cycle linking earth history, ecosystem dynamics and land use through biological ice nucleators in the atmosphere, Glob. Change Biol., 20, 341–351, doi:10.1111/gcb.12447, 2014. 26069





ACPD
15, 26067–26088, 2015



Nyeki, S., Li, F., Weingartner, E., Streit, N., Colbeck, I., Gäggeler, H. W., and Baltensperger, U.: The background aerosol size distribution in the free troposphere: an analysis of the annual cycle at a high-alpine site, J. Geophys. Res., 103, 31749, doi:10.1029/1998JD200029, 1998. 26075

Penner, J., Andreae, M., Annegarn, H., Barrie, L., Feichter, J., Hegg, D., Jayaraman, A., Leaitch, R., Murphy, D., Nganga, J., and Pitari, G.: Climate Change 2001: The Scientific Basis: Chapter 6 Radiative Forcing of Climate Change, IPCC report, 2001. 26068

Pöhlker, C., Huffman, J. A., and Pöschl, U.: Autofluorescence of atmospheric bioaerosols – fluorescent biomolecules and potential interferences, Atmos. Meas. Tech., 5, 37–71, doi:10.5194/amt-5-37-2012, 2012. 26072, 26075

Sassen, K., DeMott, P. J., Prospero, J. M., and Poellot, M. R.: Saharan dust storms and indirect aerosol effects on clouds: CRYSTAL-FACE results, Geophys. Res. Lett., 30, 1633, doi:10.1029/2003GL017371, 2003. 26069

Stanley, W. R., Kaye, P. H., Foot, V. E., Barrington, S. J., Gallagher, M., and Gabey, A.: Continuous bioaerosol monitoring in a tropical environment using a UV fluorescence particle spectrometer, Atmos. Sci. Lett., 12, 195–199, doi:10.1002/asl.310, 2011. 26071

Weingartner, E., Nyeki, S., and Baltensperger, U.: Seasonal and diurnal variation of aerosol size distributions ($10 < D < 750$ nm) at a high-alpine site (Jungfraujoch 3580 m asl), J. Geophys. Res.-Atmos., 104, 26809–26820, 1999. 26072





ACPD
15, 26067–26088, 2015



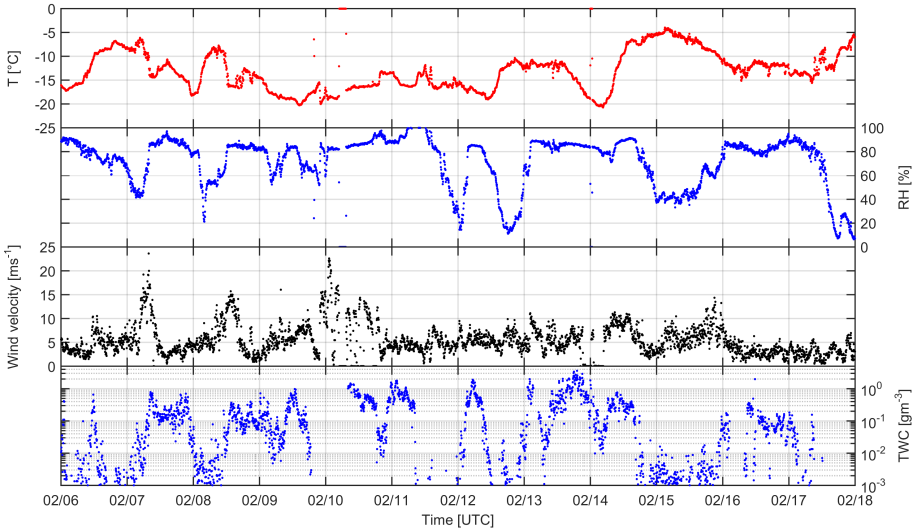


**Figure 1.** Time series of meteorological data and total water content at the JFJ site for the period 6–18 February.





ACPD
15, 26067–26088, 2015



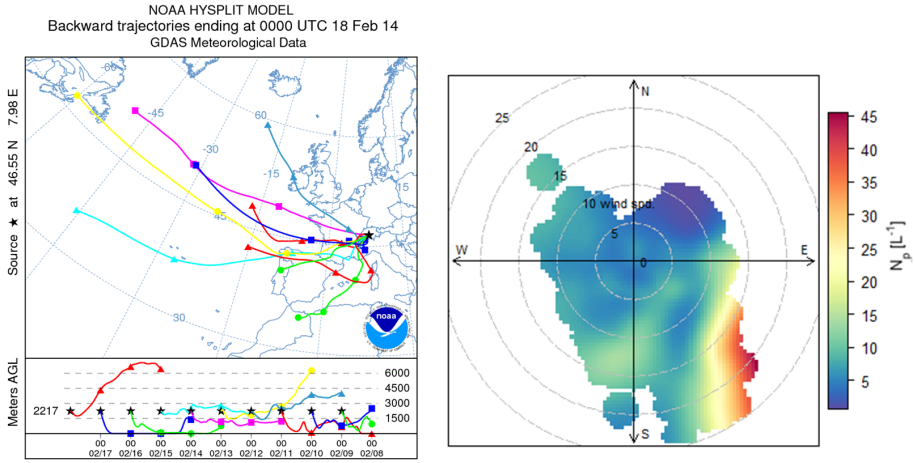


**Figure 2.** Left panel: HYSPLIT back trajectories for the period 8–18 February. Right panel: fluorescent aerosol concentration ($L^{-1}$) dependence on wind speed and direction. Wind speed denoted by concentric rings (5 m $s^{-1}$ per ring).





ACPD
15, 26067–26088, 2015



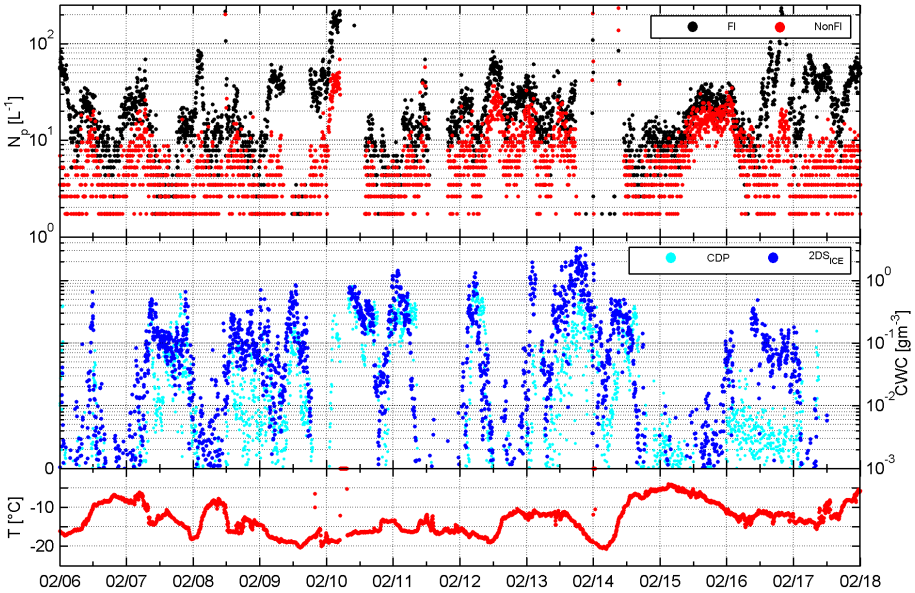


**Figure 3.** Top panel: time series of total fluorescent, $N_{FI}$, (red) and total non-fluorescent, $N_{NonFI}$, (black) aerosol concentrations measured with the WIBS-4 sampling from the total inlet (TI). Middle panel: liquid (cyan) and ice (blue) water contents measured with the CDP-100 and 3V-CPI-2DS. Bottom panel: temperature.





ACPD
15, 26067–26088, 2015



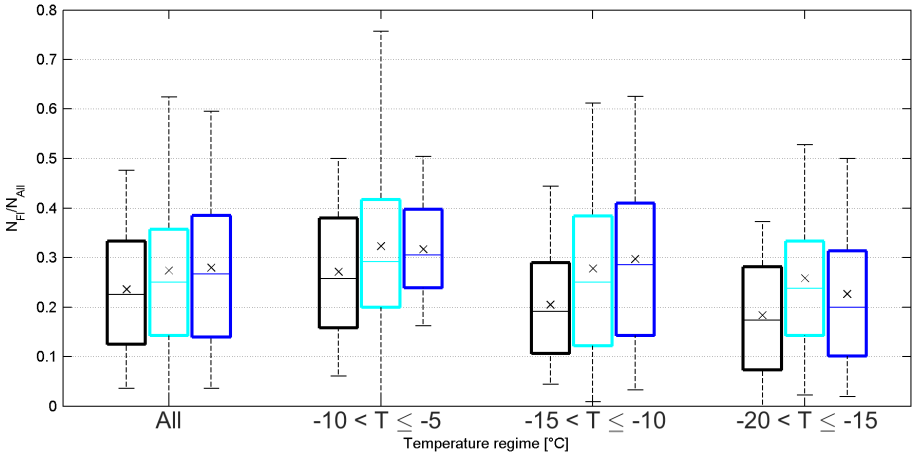


**Figure 4.** Fluorescent to total aerosol concentration ratio for out of cloud (black, TWC < 0.01 g m$^{-3}$), mixed phase (cyan, TWC ≥ 0.01 g m$^{-3}$ and IMF < 0.5) and glaciated (blue, TWC ≥ 0.01 g m$^{-3}$ and IMF ≥ 0.5) conditions sampled with the total inlet. x marker denotes mean.





ACPD
15, 26067–26088, 2015



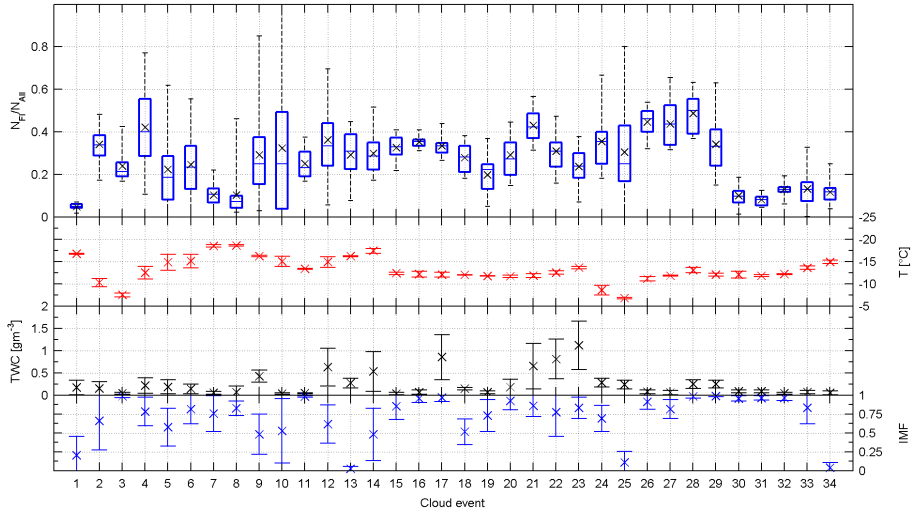


**Figure 5.** Box and whisker plots of fluorescent to total aerosol concentration ratio for cloud events persisting for at least 30 min in duration with accompanying temperature, total water content and ice mass fraction measurements. x marker denotes mean.





ACPD
15, 26067–26088, 2015



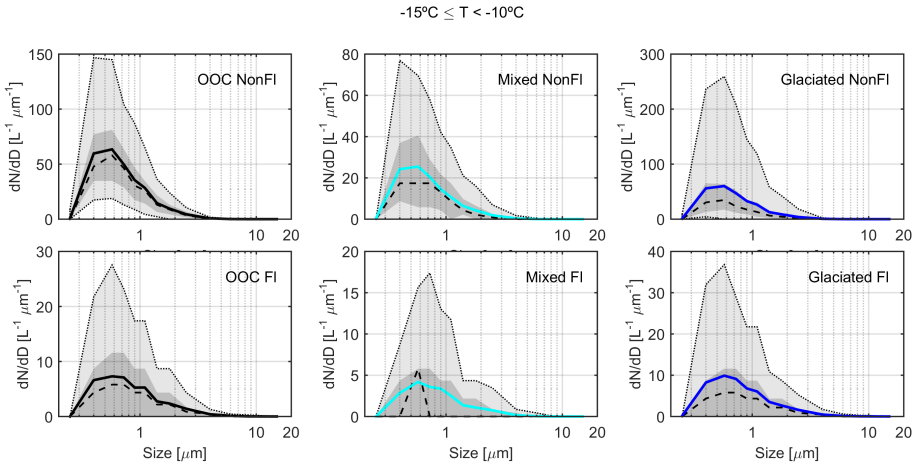


**Figure 6.** Non-fluorescent (top) and fluorescent particle size distributions (bottom) for (left to right) out of cloud (OOC), mixed phase and glaciated conditions over the temperature range $-15 < T \leq -10\,^{\circ}\mathrm{C}$. Solid line is mean, dashed line is median. 5th–95th percentiles and interquartile range shown with light and dark grey areas respectively.





ACPD
15, 26067–26088, 2015



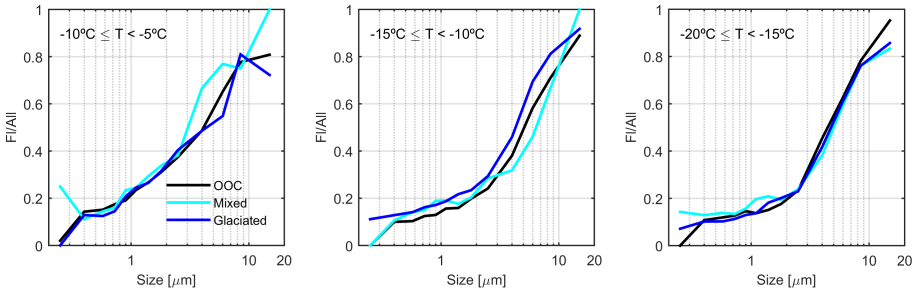


**Figure 7.** Size dependent fluorescent aerosol fractions for (left to right) out of cloud (black), mixed phase (cyan) and glaciated conditions (blue) over the three different temperature regimes studied.





ACPD
15, 26067–26088, 2015



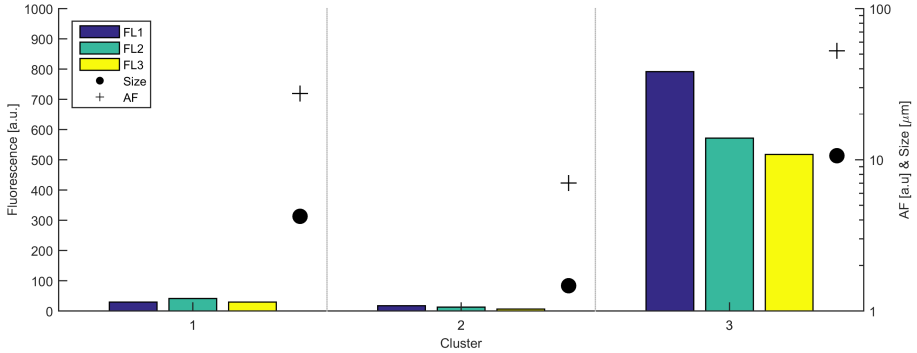


**Figure 8.** Mean cluster centres for the 3 cluster solution using Ward linkage and Calinski–Harabasz metric. Clusters contribute 25, 70 and 5 % respectively to the fluorescent particle population.





ACPD
15, 26067–26088, 2015